ISBN: 978-3-95450-261-5 ISSN: 2673-7000 doi: 10.18429/JACoW-NAPAC2025-THP066

RADIOISOTOPE PRODUCTION AT THE SPALLATION NEUTRON SOURCE: DESIGN CONCEPT OF ISOTOPE PRODUCTION TARGET *

Y. Lee†, S. H. Kim, S. Cousineau, J. Griswold
Oak Ridge National Laboratory, Oak Ridge, TN, USA

Abstract

Upon completion of the Second Target Station (STS) Project in the mid 2030s, the Spallation Neutron Source accelerator at Oak Ridge National Laboratory will deliver a 2.7 MW proton beam to the neutron production targets. In the post-STS phase, the accelerator will have a reserve beam power capacity of at least 100 kW beyond what the two neutron production targets will receive, which could potentially be ramped up to 300 kW. In this paper, a design concept for a radioisotope production target that could utilize 250 kW of the reserve beam power capacity is presented. The target consists of thorium discs encapsulated in 316L austenitic steel shells that are cooled by water. The estimated post-irradiation activity of Ac-225 and Ra-225, critical medical radioisotopes used in targeted alpha therapy cancer treatment, is calculated at the end of bombardment after a 14 day long irradiation time. Thermal and structural analyses are performed on the basis of calculated nuclear heating data. The technical feasibility of a high-power target under a 250-kW beam load with an extremely low duty factor of $3.5 \cdot 10^{-6}$ is presented from thermal, structural, and fatigue lifetime perspectives.

INTRODUCTION

With the completion of the Proton Power Upgrade (PPU) Project of the Spallation Neutron Source (SNS) at Oak Ridge National Laboratory (ORNL) [1], the SNS accelerator will be able to send 1.3 GeV proton beam to the first and second target stations at a beam pulse repetition rate of 60 Hz with a pulse energy of up to 50 kJ$\cdot$pulse^{-1}. As the first and second target stations are designed to operate at 2 MW and 700 kW respectively, the SNS accelerator will have up to 300 kW reserve beam power that can be utilized for other applications than neutron production.

Among many applications, the 1.3 GeV protons can be used to produce radioisotopes of clinical importance. In this paper, we explore the feasibility of medical isotope production using 250 kW of the reserve beam power. As a study case, a thorium target is considered for the production of Ac-225 and Ra-225 which is used as a generator for Ac-225. Ac-225 is a candidate material for targeted alpha therapy (TAT) with increasing future demand with anticipated supply shortage [2, 3].

In the current configuration of the SNS linear accelerator (LINAC), there is no available extraction beamline suitable for long pulse applications. A more feasible solution would be to construct a new beamline extending from the future Ring to Second Target (RTST) beamline as shown in Fig. 1. A radioisotope production target in this area will receive short pulse beams extracted from the accumulator ring. Challenges with the 250 kW radioisotope production target design for this scenario are the high beam pulse energy and short pulse structure of the SNS beam with a pulse length of 700 ns. In this paper, we show the feasibility of a 250 kW radioisotope production target concept that is under a high dynamic beam load with an extremely low duty factor of $3.5 \cdot 10^{-6}$ by performing particle transport, thermal, and mechanical simulations.

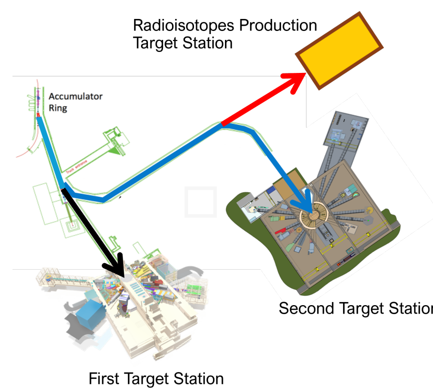

Figure 1: Potential location of the radioisotope production target station at SNS.

TARGET CONCEPT

We consider a target for the Radioisotope Production at the Spallation Neutron Source (RIPS) that receives a 1.3 GeV proton beam at a repetition rate of 5 Hz with a beam pulse energy of 50 kJ. The beam profile on the target is approximated by a super-Gaussian function, where the beam current density on the target is described by

$$i_{\text{proton}} = \frac{I_{\text{proton}}}{2\sqrt{2}\,\Gamma(\frac{1}{4})^2\,\sigma_x\,\sigma_y} \exp\left[-\frac{1}{2}\left(\frac{x^4}{\sigma_x^4}+\frac{y^4}{\sigma_y^4}\right)\right], \quad (1)$$

where I_{proton} is the proton current. The peak current density of the super-Gaussian beam is only a fraction of a Gaussian beam with the same proton current and standard deviations. A super-Gaussian beam on the target can be realized by using

* Notice: This manuscript has been authored by UT-Battelle, LLC, under contract DE-AC05-00OR22725 with the US Department of Energy (DOE). The US government retains and the publisher, by accepting the article for publication, acknowledges that the US government retains a nonexclusive, paid-up, irrevocable, worldwide license to publish or reproduce the published form of this manuscript, or allow others to do so, for US government purposes. DOE will provide public access to these results of federally sponsored research in accordance with the DOE Public Access Plan (https://www.energy.gov/doe-public-access-plan).

† leey1@ornl.gov

ISBN: 978-3-95450-261-5 ISSN: 2673-7000 doi: 10.18429/JACoW-NAPAC2025-THP066

nonlinear beam optics of octupole magnets as studied for STS beam physics [4]. For thermal and mechanical analyses presented in this paper used $\sigma_x = \sigma_y = 20$ mm which has a Full Width Half Maximum (FWHM) of 43.4 mm.

The RIPS target material has a thin disc shape. The diameter of the target disc was chosen to be 60 mm. The thickness of the target disc is determined based on stress wave dynamics enabling high intensity pulsed beam on the target and the surface area to volume ratio facilitating chemical separation of medical isotopes. The maximum differential proton energy loss in thorium for an 1.3 GeV proton is calculated to be $dE \cdot dz^{-1} = 33.1$ [MeV·cm^{-1}] by FLUKA [5–7].

With a short pulse beam impinging on the thorium volume, instantaneous thermal expansion due to proton energy deposition generates stress waves that could damage the target. Coupled transient thermal and structural analyses on a 20 mm thick thorium discs showed that maximum transient tensile stress in the target is caused by longitudinal stress wave interference in the beam direction which is normal to the disc surface. The propagation velocity of longitudinal stress wave in thorium is calculated to be $c_L = 2843$ m·s^{-1}. During the pulse length of 700 ns, the longitudinal stress wave travels 2 mm. Therefore, if the thorium disc thickness is thinner than 2 mm the coherent interference of the forward traveling and reflected waves can be suppressed. The structural failure of a thorium disc during an irradiation cycle is determined by its fatigue behavior under cyclic thermo-mechanical loading by beam pulses. The fatigue endurance limit of thorium is reported to be 97 MPa [8]. Transient thermal and structural simulations have been performed to a single beam pulse for different disc thicknesses. The calculated maximum transient stress amplitude decreases as thickness reduces. The calculated stress amplitude is 180 MPa for the thickness of 2 mm. It further reduces to 146 MPa and 72 MPa for the thicknesses of 1.0 mm and 0.5 mm respectively. For this study, we take 0.5 mm to be the thorium disc thickness.

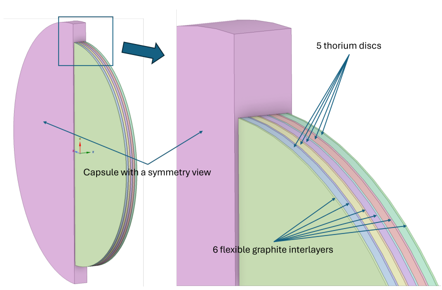

Figure 2: The layout of the thorium and flexible graphite discs in the capsule.

The 0.5 mm thin thorium discs are encapsulated in a capsule made of austenitic steel 316L. Each capsule houses 5 thorium discs. There are 0.125 mm thin flexible graphite discs between the thorium discs and capsule windows. The layout of the thorium and flexible graphite discs in the capsule is shown in Fig. 2. The beam entrance and exit windows of the capsule is 0.25 mm thick.

The capsule assemblies are placed in the cassette as shown in Fig. 3. Between the capsules, there is a 2.25 mm wide gap for coolant water flow. Note that there are openings on the side of the cassette for water inflows and outflows.

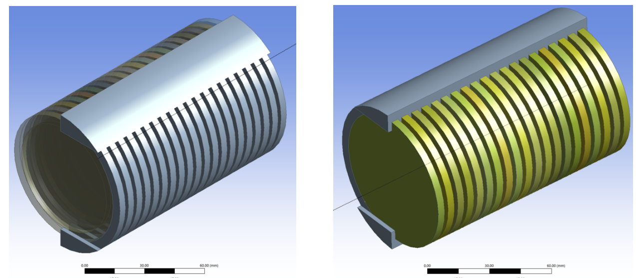

Figure 3: Target capsules placed in the cassette where only half of the symmetry volume is shown for the cassette.

Target cassette assemblies are plugged into the target vessels and the vessel volume will be closed by welding. Twenty capsule assemblies will be housed in each of the two target vessels. The choice of two separate vessels provides flexibility for different irradiation times on each vessel. Though only thorium is considered as target material for this study, other target materials can be used for producing isotopes with different application purposes, which often requires different irradiation times. Figure 4 shows the half symmetry volume of the vessels with cassettes placed inside.

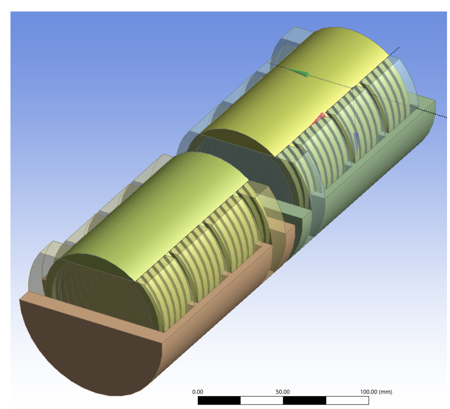

Figure 4: The half symmetry volume of the vessels with cassettes placed inside.

Figure 5 shows the water manifold of the coolant flow for a target vessel. Water flows through the 2.5 mm wide gaps between the target capsules. The height of the channel flow is 60 mm. A single channel flow enters the vessel and then splits into three parallel flows cooling the target discs, which then flows to the outlet after making six 180 degree turns. A mass flow rate of $\dot{m}$ =1 kg·s^{-1} is considered for this study. The water manifold presented is a design concept which will be optimized in future studies. Shown in Fig. 5 is the wall heat transfer coefficient configurations at the fluid-solid interfaces. The area averaged value is 17.5 kW·m^{-2}·K^{-1}.

ISBN: 978-3-95450-261-5 ISSN: 2673-7000 doi: 10.18429/JACoW-NAPAC2025-THP066

Steady thermal simulations of a capsule using a marginally reduced wall heat transfer coefficient of 14.2 $kW{\cdot}m^{-2}{\cdot}K^{-1}$ showed that the maximum temperature of the capsule surface contacting water is 55 °C which is far below the boiling point. The water flow will be optimized for more efficient cooling and reduced pressure drop in future studies.

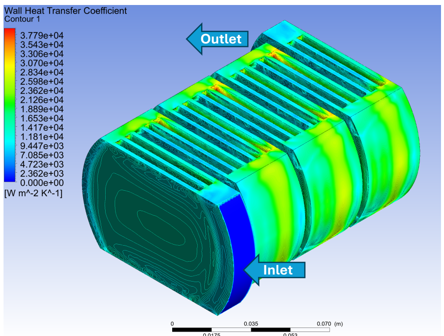

Figure 5: The water manifold of the coolant flow for a target vessel. Shown is the wall heat transfer coefficient configurations at the fluid-solid interfaces.

TARGET LIFETIME

For the production of Ac-225 and Ra-225 from the irradiated thorium target, 2 weeks per run cycle is assumed in this study, which is about the decay half-life of Ra-225. Per operational year, 12 run cycles are assumed. The whole target assembly is required to keep its structural integrity during a single run cycle. The beam entrance window (BEW) of the upstream vessel will get a maximum displacement damage of 0.4 dpa during a single run cycle at which 316L still retains >50% of total elongation [9]. In the vessel, the BEW will get the highest fatigue loads, and the design of this part should be optimized to endure $1.0{\cdot}10^8$ beam pulses. We defer the structural optimization of the vessel to future works. Here, we address the issue whether the capsule assemblies can endure a two-week long single run cycle.

Steady thermal and structural analyses have been performed. The water pressure provides an estimated thermal contact resistances of 10^{-4} $m^2{\cdot}K{\cdot}W^{-1}$ at the contact surfaces of flexible graphite and other solids [10]. The calculated steady peak maximum principal stresses in the capsule is 163 MPa which is about 30% of the ultimate tensile strength of the 316L stainless steel. The maximum stress is caused by bending at the interface between the capsule rim and window. The steady peak maximum principal stress in the thorium disc is 2.2 MPa which is less than 1% of the yield strength. Flexible graphite discs are used as functional material and these are mostly in compression.

Transient thermal and structural analyses have been performed for a single pulse with 100 µs post-pulse duration to estimate the fatigue factor of safety of the capsule and the thorium discs. The calculated strain amplitude of the capsule is 0.04% which is less than the fatigue limit of 0.1% for $1.0{\cdot}10^7$ load cycles [11]. Figure 6 shows the strain response of the target capsule to a single beam pulse. The calculated

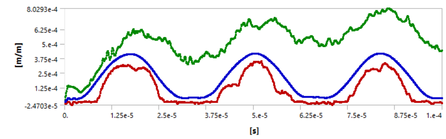

Figure 6: The strain response of the target capsule to a single beam pulse. Shown are the maximum, average and minimum values of the maximum principal elastic strain.

stress amplitude of the thorium disc is 36 MPa, which is about 37% of the fatigue endurance limit. This indicates that the thorium discs will endure the beam pulse induced fatigue load cycle during a 14 day long run cycle.

ISOTOPES YIELDS

A FLUKA model has been performed for the target model described from Fig. 2 to Fig. 5. Figure 7 shows the calculated yields of Ra-225 and Ac-225 at the end of a two-week long proton bombardment (EOB) on the target with a time averaged proton rate of $1.2{\cdot}10^{15}$ $protons{\cdot}s^{-1}$. The total EOB

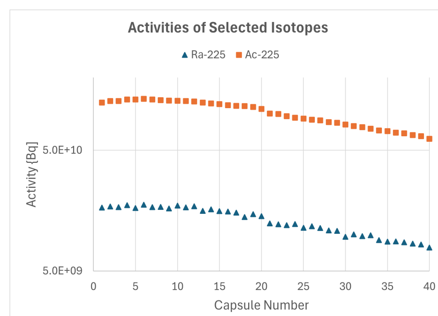

Figure 7: The EOB yields of Ra-225, Ac-225 and Ac-227 yields in each target capsule.

activities of Ra-225 and Ac-225 are 0.53 TBq and 4.12 TBq respectively. For reference, each TBq of Ra-225 can generate 0.9 TBq of Ac-225 assuming a week long operational cycle of the generator [12]. It is estimated that Ac-225 that can be separated from the thorium target irradiated for a single run cycle could serve for about 100,000 patient doses [12, 13].

CONCLUSIONS

This paper presents a design concept for a medical isotope production target using the 1.3 GeV protons at SNS. Computational analyses indicate that the target could potentially withstand 50 $kJ{\cdot}s^{-1}$ beam pulse energy with 5 Hz repetition rate for a two-week production run cycle. The target capsules can house any medical isotope production target materials depending on the needs. A thorium target was considered for the feasibility study presented. Thanks to the long interaction range of the 1.3 GeV protons in the target, the Ac-225 activities that can be produced from the thorium target in a single run cycle is estimated to serve about 100,000 patient doses, theoretically. Future work will be dedicated to designing a target station with shielding, radioactive material cells and remote handling equipment.

ISBN: 978-3-95450-261-5 ISSN: 2673-7000 doi: 10.18429/JACoW-NAPAC2025-THP066

REFERENCES

[1] F. C. Pilat, "SNS upgrade and power ramp up", Presented at the ICFA Adv. Beam Dyn. Workshop High-Intensity High-Brightness Hadron Beams (HB'23), Geneva, Switzerland, Oct. 2023, paper THC1I1, unpublished.

[2] V. Radchenko *et al.*, "Production and supply of α-particle–emitting radionuclides for targeted α-therapy", *J. Nucl. Med.*, vol. 62, pp. 1495–1503, 2021. doi:10.2967/jnumed.120.261016

[3] A. K. H. Robertson, C. F. Ramogida, P. Schaffer, and V. Radchenko, "Development of 225Ac radiopharmaceuticals: TRIUMF perspectives and experiences", *Curr. Radiopharm.*, vol. 11, no. 3, pp. 156–172, Oct. 2018. doi:10.2174/1874471011666180416161908

[4] A. P. Shishlo, private communication, 2022.

[5] FLUKA, https://fluka.cern

[6] G. Battistoni *et al.*, "Overview of the FLUKA code", *Ann. Nucl. Energy*, vol. 82, pp. 10–18, 2015. doi:10.1016/j.anucene.2014.11.007

[7] C. Ahdida *et al.*, "New capabilities of the FLUKA multi-purpose code", *Front. Phys.*, vol. 9, p. 788253, 2022. doi:10.3389/fphy.2021.788253

[8] MatWeb, Thorium, Th, MATERIAL PROPERTY DATA, https://www.matweb.com

[9] D. A. McClintock *et al.*, "Characterization of mechanical properties and deformation behavior of highly irradiated 316L stainless steel from target modules at the Spallation Neutron Source using digital image correlation analysis", *J. Nucl. Mater.*, vol. 545, p. 152729, 2021. doi:10.1016/j.jnucmat.2020.152729

[10] E. E. Marotta, S. J. Mazzuca and J. Norley, "Thermal joint conductance for flexible graphite materials: Analytical and experimental study", *IEEE Trans. Compon. Packag. Technol.*, vol. 28, No. 1, pp. 102-110, 2005. doi:10.1109/TCAPT.2004.843153

[11] AFCEN, *RCC-MRx: Design and Construction Rules for Mechanical Components of Nuclear Installations*, Paris, France: Association Française pour les règles de Conception et de Construction des Matériels des Chaudières Electro-nucléaires (AFCEN), 2012.

[12] A. K. H. Robertson *et al.*, "^{232}Th-spallation-produced ^{225}Ac with eeduced ^{227}Ac content", *Inorg. Chem.*, vol. 59, no. 17, pp. 12156-12165, 2020. doi:10.1021/acs.inorgchem.0c01081

[13] H. Rathke *et al.*, "Deescalated ^{225}Ac-PSMA-617 versus ^{177}Lu/^{225}Ac-PSMA-617 cocktail therapy: A single-center retrospective analysis of 233 patients", *J. Nucl. Med.*, vol. 65, pp. 1057–1063, 2024. doi::10.2967/jnumed.123.267206